IRCS: Infrared Camera and Spectrograph for the Subaru Telescope

Naoto Kobayashi[a], Alan Tokunaga[b], Hiroshi Terada[c], Miwa Goto[c], Mark Weber[a], Robert Potter[a]
Peter Onaka[b], Gregory Ching[b], Tony Young[b], Kent Fletcher[b], Douglas Neil[b], Louis Robertson[b]
Daniel Cook[b], Masatoshi Imanishi[b], David Warren[d]

[a]Subaru Telescope, National Astronomical Observatory of Japan,
650 North A'ohoku Place, Hilo, Hawaii 96720, USA
[b]Institute for Astronomy, University of Hawaii, 2680 Woodlawn Drive,
Honolulu, Hawaii 96822, USA
[c]Department of Physics, Faculty of Science, Kyoto University,
Kitashirakawa, Sakyo-ku, Kyoto 606-8502, Japan
[d]The Aerospace Corporation, M4-978, P.O. Box 92957,
Los Angeles, California 90009, USA

ABSTRACT

We report current status of the Infrared Camera and Spectrograph (IRCS) for the Subaru Telescope. IRCS is a Subaru facility instrument optimized for high-resolution images with adaptive optics (AO) and tip-tilt at 1−5μm. IRCS consists of two parts: one is a cross-dispersed spectrograph providing mid to high spectral resolution (R=5,000−20,000), the other is a near-infrared camera with two pixel scales (0.058, 0.023 arcsec/pix), which also serves as an infrared slit-viewer for the echelle spectrograph. The camera also has grisms for low to medium resolution (R=100−1,000) spectroscopy. We have just completed the first engineering run about one month before this SPIE conference. It was an initial performance evaluation without AO or tip-tilt to check IRCS and its interface to the telescope. We confirmed the basic imaging and spectroscopic capability we had estimated.

Keywords: infrared, near-infrared, camera, spectrograph, imaging, imager, spectroscopy, adaptive optics, tip-tilt, Subaru Telescope

1. INTRODUCTION

Deep near-infrared imaging and spectroscopy are essential functions of 8-m class telescope for key sciences like cosmology, galaxy formation,[1] and planet formation.[2] The capability of ground-based near-infrared observation has been significantly improved these five years thanks to the large aperture telescopes with diffraction-limited image quality as well as large-format cutting-edge infrared arrays.[3] A number of state-of-art near-infrared spectrographs are being built for 8−10m telescopes[4–6] and IRCS is one of them for the Japanese 8.2-m Subaru Telescope.[7]

Subaru Telescope, which started an engineering operation from January 1999, was proved to have an excellent image quality and frequently delivers 0″.3 seeing images in the near-infrared.[8] Thus, the adaptive optics (AO) system[9] or tip-tilt system is expected to deliver sharp images with high Strehl ratio constantly. To make most of this image quality, IRCS was specifically optimized for AO and tip-tilt with fine pixel scales (0″.023−0″.075) and narrow slits (0″.1−0″.3). Since near-infrared observations are usually background-limited, AO/tip-tilt imaging also significantly improves sensitivity both for imaging and spectroscopy.

2. INSTRUMENT DESIGN AND SPECIFICATION

The detailed design features of IRCS optics, mechanisms and electronics are described in Ref. 7,10–13. The current specifications are summarized in Tables 1–3.

Further author information: (Send correspondence to NK)
NK: E-mail: naoto@subaru.naoj.org

Table 1. IRCS: **Imaging**

Pixel scales	0″.058/pix (F.O.V.∼ 60″) for tip-tilt†
	0″.023/pix (F.O.V.∼ 25″) for AO
Filters (broad-band)	J,H,K,K',L',M', ND filter(1%), PK50 thermal blocker
	− planned to be installed −
	H+K', coated thermal blocker
Filters (narrow-band)	Brγ, K-continuum, [FeII]1.64 μm, H-continuum
	− planned to be installed −
	H_2 v=1-0 S(0), H_2 v=1-0 S(1), CO v=2-0 bandhead,
	Hydrocarbon(3.3 μm), Brα, L-continuum
	Paβ, J-continuum

†: also for w/o image correction.

Table 2. IRCS: **Echelle Spectroscopy**[a]

Pixel Scale		0″.075/pix				
Slit Width		0″.15, 0″.30, 0″.60				
Wavelength Range		Resolving Power[b]	Slit Length	Required Exposures[c]	Echelle Orders	Cross-disperser Orders
zJ	(1.03−1.18 μm)	19,000−22,600	3″.8	1	56−48	6
J	(1.18−1.38 μm)	19,000−22,600	3″.8	1	47−42	5
H	(1.49−1.83 μm)	18,800−22,900	5″.6	2	38−32	4
K	(1.90−2.49 μm)	18,300−23,600	7″.3	2	29−23	3
L	(2.90−4.16 μm)[d]	17,300−25,100	10″.0	6	19−14	2
M	(4.41−5.34 μm)	16,800−26,300	10″.0	4	12−11	1

[a] The imager (either 58 or 23 mas/pix) serves as an infrared slit-viewer in this mode.
[b] For 0″.15-slit. The resolving power reduced by 0.5 and 0.25 for 0″.3- and 0″.6-slits, respectively.
[c] Number of exposures to cover the entire wavelength range shown in the left-most column.
[d] As of March 2000, this mode is not availabe because the order-sorting filter is not installed.

3. INTEGRATION AND TESTING

IRCS was developed by a collaboration of the Institute for Astronomy (IfA), University of Hawaii, and the National Astronomical Observatory of Japan (NAOJ) with funding from NAOJ. All the development work, design and fabrication, were done at the IfA in Honolulu. Some major components (e.g., four mirror anastigmat, Offner relay) were designed, assembled, and cryogenically tested at outside companies and delivered to the IfA. All the other mechanical design, machining and electronics were done in house.

After the completion of the cryostat, major mechanisms, and electronics, we conducted cooldown tests with a bare multiplexer at IfA to confirm their cryogenic performance. Testing of two science grade arrays were done separately using a test cryostat at IfA.[13] After those initial performance checking, the IRCS was delivered to the Subaru Hilo facility in March 1999. An extensive optical alignment of both camera/spectrograph was conducted with four cooldown cycles at the Subaru Hilo facility. Two arrays were installed and their cryogenic performance was confirmed. The cryostat and all the electronics boxes were installed into an instrument container of size 2m×2m×2m following the Subaru instrument container guideline.[14] Using the telescope simulator in the Hilo facility,[14] we checked various interfaces to the telescope and the flexure of the entire IRCS assembly. Major achievements of the

Table 3. IRCS: **Grism Spectroscopy**

Pixel Scale	0″.058/pix
Slit Width	0″.15, 0″.30, 0″.60, 0″.90
Slit Length	∼20″

Wavelength Range		Resolving Power[a]	Required Exposures	Grism Order	Grism
J+H	(1.0−1.6 μm)[b]	∼200 (ave.)	1	1	No.3
Iz	(0.92−1.01 μm)	650−720	1	7	No.1
zJ	(1.03−1.18 μm)	650−740	1	6	No.1
J	(1.18−1.38 μm)	630−720	1	5	No.1
H	(1.49−1.83 μm)	620−760	1	4	No.1
K	(1.90−2.49 μm)	620−800	1	3	No.1
L	(2.90−4.16 μm)[b]	350−500	1	1	No.4

[a] For 0″.30-slit. The resolving power is double for 0″.15-slit while reduced by 0.5 and 0.33 for 0″.6- and 0″.9-slits, respectively.
[b] As of March 2000, these modes are not available because the order-sorting filters are not installed.

Pixel Scale	0″.023/pix
Slit Width	0″.10, 0″.15, 0″.30
Slit Length	∼20″

Wavelength Range		Resolving Power[c]	Required Exposures	Grism Order	Grism
Iz	(0.92−1.01 μm)	560−620	1	7	No.2
zJ	(1.03−1.18 μm)	560−650	1	6	No.2
J	(1.18−1.38 μm)	550−720	1	5	No.2
H	(1.49−1.83 μm)	550−660	1	4	No.2
K	(1.90−2.49 μm)	550−700	1	3	No.2

[c] For 0″.15-slit. The resolving power is increased by 1.5 for 0″.10-slit while reduced by 0.5 for 0″.3-slit.

laboratory integration and testing are summarized in the following sections.

3.1. Optics

3.1.1. Fore-optics

A 1–5.5 μm infrared-transmissive cryogenic beamsplitter (0.6–0.8 μm visible-reflective) was installed to deliver visible light to the wave-front-sensor of the Subaru AO system.[9] It was designed and coated by Thin Film Lab. (Milford, PA) on a CaF_2 substrate of 10 mm thickness by Janos, Inc. (Townshend, Vermont). The transmittance at 1–5.5 μm is an average of 95% and the reflectance in visible wavelengths is more than 98%. An AR-coated CaF_2 flat of the same thickness is inserted after the beamsplitter to compensate for the astigmatism due to the beamsplitter. The durability of the coating was confirmed with ten thermal cycles between the room temperature and the liquid nitrogen temperature. Since the beamsplitter and the compensator are inserted in converging beam near the focal plane, two low-level elliptical ghosts from each optics appear at approximately 17″ distance for bright objects.

An Offner relay is used to re-image the telescope focal plane onto the spectrograph slit. The Offner relay was designed, manufactured, and cryogenically tested at Applied Physics Specialties (Don Mills, Ontario, Canada). It

Table 4. IRCS: **Grisms**

Grism	Pixel Scale	Wavelength Range	Grooves [lines/mm]	Blaze Angle [degree]	Prism Angle [degree]	Substrate	Type	Manufacturer
No.1	58 mas	1−2.5 μm	40	26.7	30.5	ULTRAN30	replica	RGL[a]
No.2	23 mas	1−2.5 μm	20	13.0	14.75	ULTRAN30	replica	RGL[a]
No.3	58 mas	1−2.5 μm	75	10.0	12.5	ULTRAN30	replica	RGL[a]
No.4	58 mas	2.8−4.2 μm	54.25	7.85	7.85	KRS-5	direct ruling	Carl-Zeiss[b]

[a] Richardson Grating Laboratory, Spectronic Instruments (Rochester, New York)
[b] Carl Zeiss Jena GmbH (Jena, Germany)

has a nickel-coated and polished aluminum primary and a bare aluminum diamond-turned secondary. The wave-front error is roughly $1/2\lambda$ peak-to-peak at 0.6 μm.

3.1.2. Camera

All the lenses (BaF_2, LiF, ZnS, ZnSe) were manufactured and coated by Optics for Research Inc. (Caldwell, NJ), Thin Film Lab., respectively. The average transmittance of the coating is 97% in 1−5.5 μm per surface. All the reflective flat mirrors were made of fused-silica by Optics for Research and protective-silver coated by Denton Vacuum (Moorestown, NJ), showing more than 98% transmittance throughout 1−5.5 μm per surface.

The broad-band filters (J,H,K,K',L',M') were made by the near-infrared filter consortium organized by A. Tokunaga (see http://www.ifa.hawaii.edu/~tokunaga/) and D. Simons[15,16] (see Table 1). All these filters were manufactured by OCLI (Santa Rosa, CA). Currently only four narrow-band filters are installed, but twelve narrow-band filters can be installed in total. IR Engineering (Maldon, Essex, England) fabricated the narrow-band filters.

Four grisms are installed as shown in Table 4. We plan to install two more grisms (one for H+K-band low-resolution spectroscopy, the other is under discussion) in the future. The grisms No.1 & No.2 are used in 3rd order (K band), 4th order (H band), 5th order (J band), 6th order (zJ band), and 7th order (Iz band) as shown in Figure 1. Order-sorting filters were made at IR Engineering and one remaining filter (L band) is currently under fabrication at the company. Since some of the order-sorting filters as well as narrow-band filters have a thermal leak of order of few $\times 10^{-4}$ at around 4 μm, a thermal blocker (e.g., PK50 blocker) has to be inserted.

Since the light beam is reflected to the camera section at the focus of the Offner relay, we use a "reflective" slit for grism spectroscopy. The concept and design of the reflective slits are described in Ref. 10. We put a flat mirror behind the reflective slit to reflect the light which falls on the sides of the slits back to the telescope. It turned out that this back mirror suppresses scattering and ghost from the background of the reflective slit very well. A detail analysis of scattering from the slit surface is underway, but we do not see any serious problem so far.

3.1.3. Spectrograph

The collimator of the spectrograph is an off-axis aluminum parabola with a 300 mm focal length. It was first diamond-turned at Applied Physics Specialties and later polished by SSG Inc. (Wilmington, MA). The surface quality is $1/5\lambda >$ (peak-to-peak), which meets our specification. The four mirror anastigmat (FMA), which consists of two spherical and two aspheric aluminum mirrors, was designed, manufactured, aligned, and cryogenically tested at SSG, Inc. The wavefront error of the entire system was measured at $1/5\lambda$ (rms) both in room temperature and cryogenic temperature, and the overall performance of FMA was quite satisfactory.

Two gratings (echelle and cross-disperser) were manufactured by Hyperfine, Inc. (Boulder, Colorado). Those are replica gratings on aluminum substrates. We found some Lyman or Rowland ghosts from the echelle grating using a strong Ar line in H-band, but it is very low (less than 1×10^{-4}) and that proves the excellent performance of this grating. The same order-sorting filters as for the grism spectroscopy are used (see Figure 1). Although we cannot put a thermal blocker in the spectrograph (we have only one filter wheel), any thermal leak of the filters is dispersed out of the beam and does not affect the spectrum on the array.

3.2. Optical alignment

The camera side alignment was mainly done using a Taylor Hobson Inc. (Rolling Meadows, Illinois) alignment telescope. Each lens mount has a flat alignment surface whose center is identical to the optical axis at cryogenic temperature. Each mount was aligned to a given optical axis using a Taylor Hobson standard circular target attached to the alignment surface. The camera image quality was checked using chrome-coated Ronchi targets installed in the slit wheel (focal plane). The MTF at a spatial frequency of 8.3 cycles/mm (4-pixels for 58 mas camera) was measured and confirmed to be correct from ray-tracing. The spectral resolution of the grism spectra was confirmed using Ar lines.

On the spectrograph side, a shear-interferometer was used to check the collimation of the beam after the collimator. The FMA unit was installed and aligned to the optical axis of the collimator using laser and a pin-hole in the slit wheel. We confirmed the resolving power of the spectrograph using Ar lines at various locations on the array.

3.3. Baffling

All the optical paths are enclosed in aluminum baffle tubes which are painted black. In the laboratory, we could not detect any significant light leak or stray light for both camera and spectrograph sections. This is very important for our application since the thermal background is comparable or smaller than the detector dark current ($\sim$0.2 e^-/sec) for high resolution spectroscopy.

3.4. Cryostat

The cryostat vacuum is 1×10^{-4} torr after a few days of pumping at the room temperature. The vacuum on the summit (e.g., 1×10^{-5} torr) since the ambient temperature is about 20 K cooler. The optical cold table is pre-cooled to 77 K with 600 liter of LN_2 in two days. Another two days are necessary to stabilize the temperature at around 65 K with Sumitomo closed-cycle cooler. The typical vacuum after the cooldown is 3×10^{-7} torr in the laboratory while it is 3×10^{-8} torr on the summit because of less out gassing from the vacuum jacket with the colder ambient temperature. The temperature gradient across the optical cold table was measured to be less than 5 K.

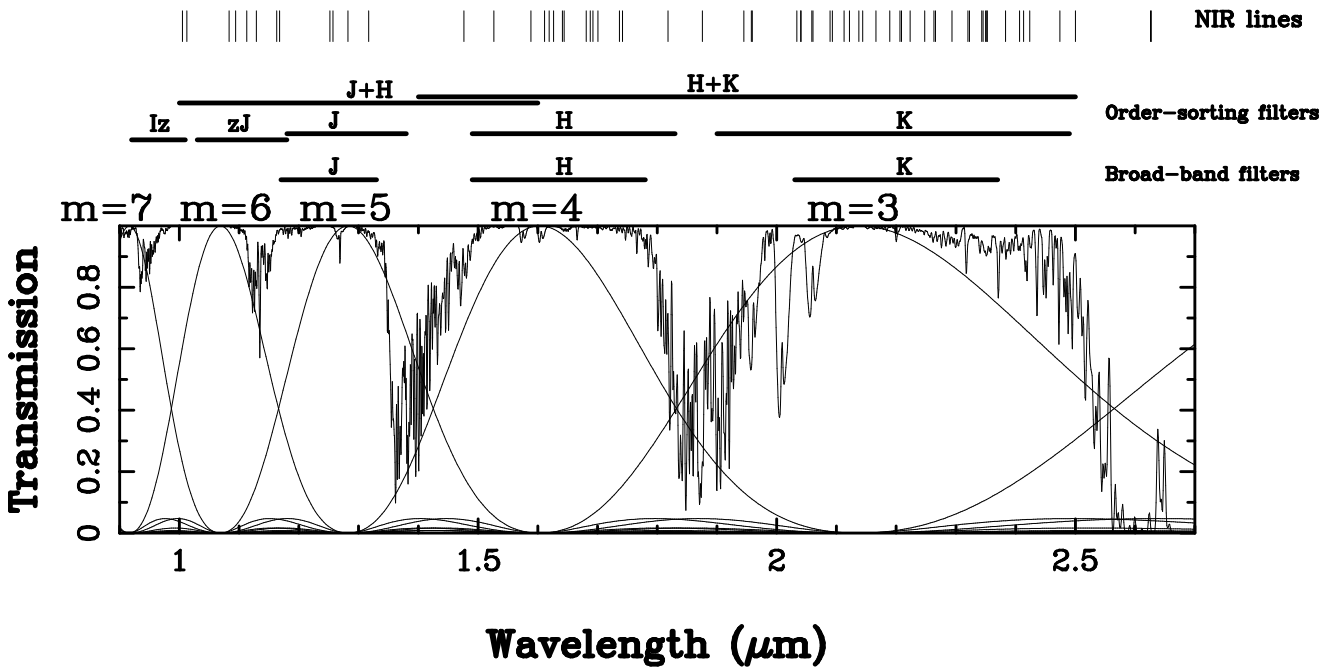

Figure 1. Theoretical efficiency curves for the grism No.1 (for 58 mas) are plotted over an atmospheric transmission curve at 0.9–2.7 μm under conditions appropriate for Mauna Kea.[17] The grism No.2 (for 23 mas) has similar efficiency curves. The wavelength coverages of order-sorting filters are also plotted. The top-most row shows known astronomical near-infrared lines.[17]

3.5. Mechanisms and Optics Mounts

All nine mechanisms designed and fabricated in house at IfA[18] show excellent performance at cryogenic temperature. The repeatability of the mechanisms in the camera section was so good that we could not measure it with our pixel scale. In the spectrograph section the two grating stages showed 1−2 pix (peak-to-peak) repeatability on the array. However, this is not a problem since calibration data is usually taken before moving those gratings. Simultaneous homing of the mechanisms can be done, which enables quite efficient mode switching.

3.6. Infrared Arrays and array electronics

IRCS uses two Raytheon (formerly SBRC) 1024×1024 InSb arrays with Aladdin II multiplexer. The camera array (SCA 48391) is a semi-science grade array which has a low average quantum efficiency of ∼40% and a large variation of quantum efficiency across the array. The spectrograph array (SCA 42821) shows good quantum efficiency (> 80%) and uniformity. Typical readnoise for both array is 55 e^- with double-sampling and ∼14 e^- with 16 non-desctuctive sampling. The typical dark current was 0.2−0.3 e^-/sec*. Typical array operating temperature is 30K. The gain was measured at 12.2 e^-/ADU for 300mV detector bias. The detail of the array readout electronics and the Subaru array performance evaluation is partly reported in Ref. 13 and will be summarized in detail elsewhere.

We have observed a noticable residual image after the electron well was filled more than 50%. Altough zero-biasing removes this residual completely, we did not use this method because it could slightly change flat-fielding, dark current, and conversion rate. A workaround is background reset and dummy readout of some frames before each exposure, which reduces the residual image reasonably well (e.g., less than 0.1%).

3.7. Mechanism control and temperature control

Cryogenic motors manufactured by Phytron-Elektronik GmbH (Gröbenzell, Germany) were used for all mechanisms with their standard motor drivers. Comprehensive performance evaluation of this cryogenic motor was done at IfA by K. Hodapp, T. Young, J. Douglass, and J. Bell. The motors work well both in the cryogenic temperature (60−80K) and room temperature. However, the motors are not moved at intermediate temperature because of differential thermal contraction of various metal parts.

The position sensing of all mechanisms were done with Hall effect sensors with custom electronics developed in house. Typical repeatability we achieved is 5−10 μm, which is much more than we expected and this demonstrates that the Hall effect sensor is an excellent alternative for absolute position sensing at cryogenic temperatures.

Temperatures at various locations were monitored using silicon diode temperature sensors by Lakeshore Inc. (Westerville, OH) with unshielded wires. The advantage of the unshielded wires is the reduction of the number of wires, but a drawback is that temperature sensors can easily pick up noise from motors. After any mechanism motion it takes typically 30 seconds to stabilize the array temperature readout.

Temperatures of the two arrays and the cold work surface are actively controlled with Lakeshore temperature controllers. If the array temperature changes by more than 0.1 K, the images tend to show not only slight DC level change (different from quadrant-to-quadrant) but also black spots of negative counts whose locations and numbers change from exposure to exposure (thus, it is called "tachyon"). With an appropriate setting of the Lakeshore controller, temperature control of 0.01 K accuracy was achieved. For the cold work surface, the heater and the temperature sensor are located on the cold strap between the cold work surface and the cooler head. Although the time constant is quite large (more than 6 hours), the temperature of the cold work surface can be controlled at the desired temperature at of 60–65K.

3.8. Software

IRCS software consists of four parts: data aquisition, mechanism control, temperature/vacuum sensor monitors, and the telescope control. All the software are integrated into a GUI ("IRCS GUI") so that we can control everything from a single top-level window (Figure 2). IRCS GUI has a Skycat† base display with WCS (world coordinate system). Telescope control can be easily done using arrows on the image display. Basic macro function is also provided.

*However, the dark current of Aladdin II array is very large for shorter integration time (<5 sec), which determines the final dark counts for typical integration time for near-infrared observations (e.g., 2 min).

†http://archive.eso.org/skycat/

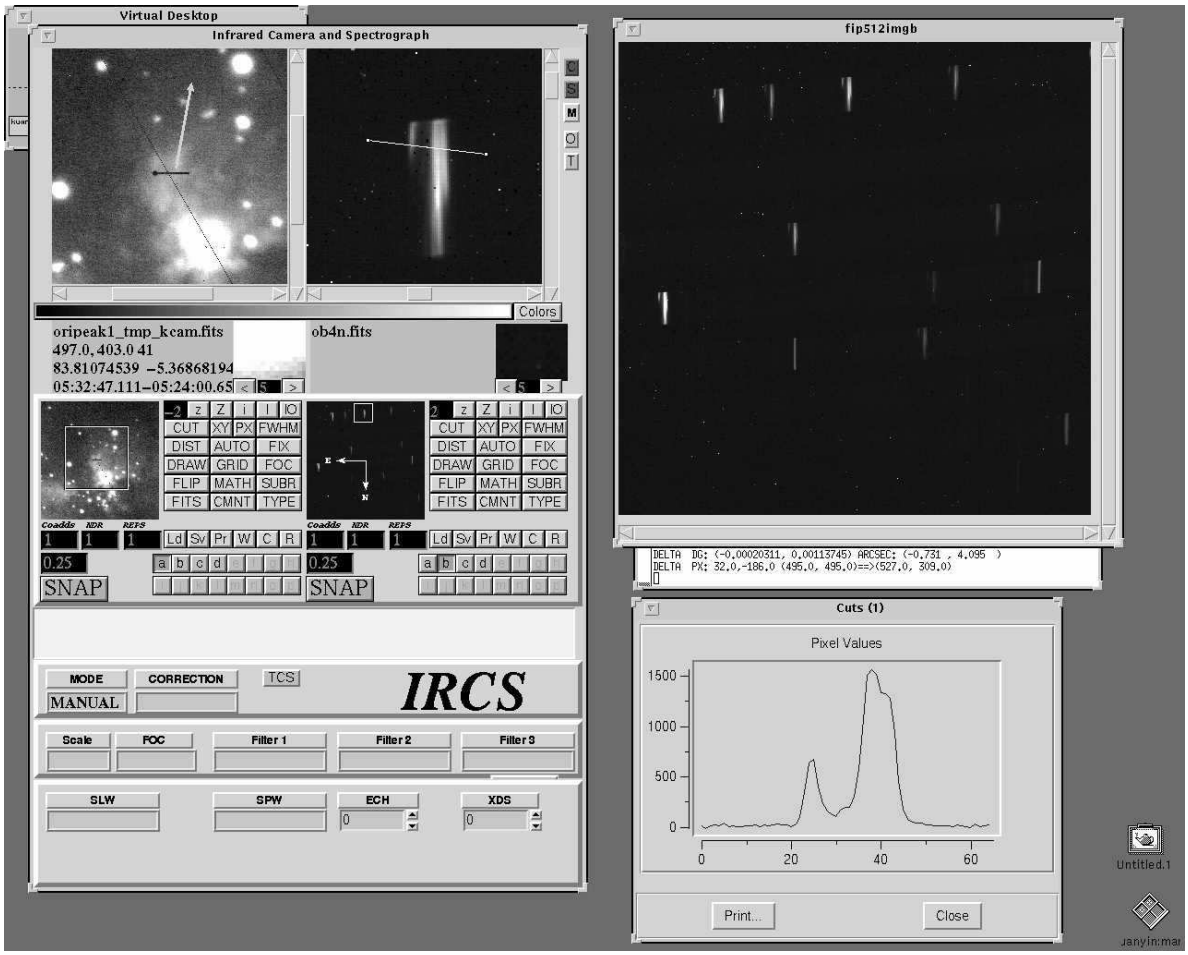

Figure 2. GUI window during observing. The left window is the top-level window of IRCS GUI. The left and right side of the GUI window show the images and control panels for the camera and spectrograph sections, respectively. Simultaneous readouts of both camera and spectrograph is possible. Quick look image processing is provided (zoom, add, subtract, divide, line cut, FWHM calculation, etc.). In this particular snapshot the camera is used as an infrared slit viewer for the echelle spectrograph.

3.9. Instrument Container and Flexure of the assembly

The IRCS cryostat and two 1m×1m×2m electronics boxes are integrated into a package called "instrument container".[14] It is 2m×2m×2m structure equipped with "automatic connectors"[14] through which all the fiber, electrical, glycol, and He gas connections to the telescope are done. The weight of the entire assembly is about 2 metric tons. Figure 3 shows fully equipped IRCS attached to the Cassegrain focus of the Subaru Telescope.

The flexure of the IRCS was measured at the telescope simulator (called "optical simulator"[14]) at the Subaru Hilo facility. It was 0″.09 (peak-to-peak) for a 45-degree elevation change and 0″.18 (peak-to-peak) for a 90-degree elevation change. The optical axis of IRCS was measured to be within 3 arcmin with respect to the normal of the top flange of the container. These numbers meet our specification.

4. FIRST ENGINEERING RUN

We have conducted a first engineering run of IRCS during 25 February to 2 March, 2000. All of the nights were photometric. Since the Subaru AO system was not yet delivered to the telescope and the tip-tilt system was still in an engineering phase, we have conducted the engineering run with only the optical secondary to check the basic

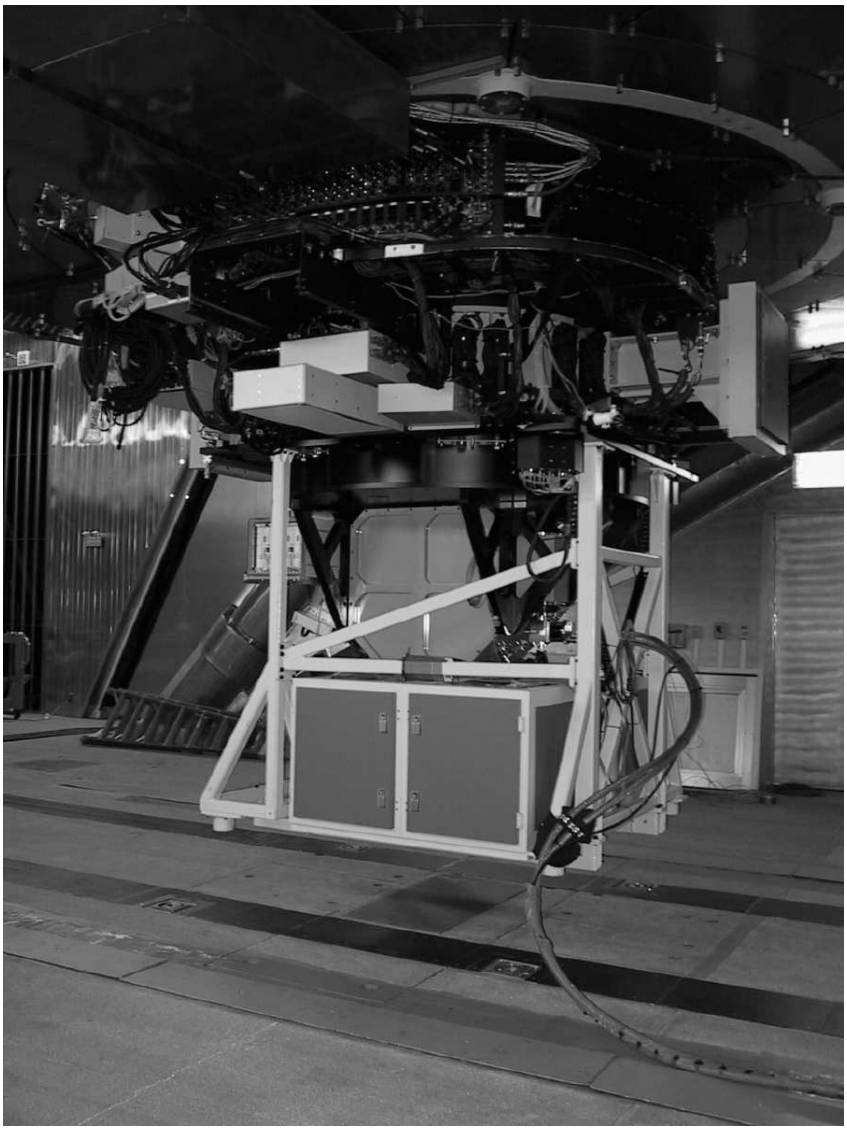

Figure 3. The IRCS attached to the Cassegrain focus of the Subaru Telescope.

performance of IRCS (image quality, throughput, and limiting magnitude) and the interface to the telescope both for hardware and software. On the whole, we confirmed that IRCS performance meets our original specification.

4.1. Imaging

During the engineering run, seeing in 2.2 μm was often $0''.3-0''.4$ with 1 sec integration time and $0''.45$ in two minutes with open loop tracking. Occassionally $0''.2-0''.3$ images with 1-sec integration time were recorded. When the seeing was not that excellent, we obtained JHK images of Persson standards[19] to establish the color correction for the new near-infrared filter system. We did not use the 23 mas camera since the pixel scale is too small under normal seeing condition.

The measured throughput of $\sim$12% (including quantum efficiency of the array) is about half that of our original specification. This is because of the low-quantum efficiency of the camera array as described in §3.6. Nevertheless, our preliminary analysis shows good sensitivity in all the broad-bands (e.g., K'=21.2 mag, 5σ, 1 hour integration time, $2''$ aperture diameter for FWHM=$0''.5$ image) primarily because the sky background counts was quite low. We

expect to get the originally specified throughput and 0.4 mag higher sensitivity after the installation of a new array at the end of this year. The emissivity of the entire system (atmosphere + telescope + instrument) was estimated at roughly 10% assuming a single temperature of 273K. This low emissivity shows that Subaru Telescope is well suited for infrared observation.

For themal-infrared (3−5 μm) imaging with the 58 mas camera, we used a sub-array (512×512 pixels which provides a 30″×30″ F.O.V.) to keep the integration time less than 0.2 seconds to avoid saturation of the array with thermal background. The minimum integration time for the entire array is 0.41 seconds[‡]. The new array we plan to install at the end of this year has an Aladdin III multiplexer which enables a faster frame readout rate, and imaging with 1024×1024 pixels in the thermal infrared will be possible.

4.2. Grism Spectroscopy

We have obtained grism spectra with the 58 mas pixel scale of some Persson standard stars and a QSO to confirm the basic performance. Since it was a seeing-limited observation, we used the 0.6-arcsec slit to maximize the number of photons through the slit. We did not see any apparent problem and confirmed that IRCS is ready for grism spectroscopy. More detailed performance evaluation is underway.

4.3. Echelle Spectroscopy

Using the narrowest slit (0.15-arcsec), we have obtained a number of high-spectral resolution (R=20,000) K-band spectra of some young stellar objects and proto planetary nebulae. Figure 4 shows the spectrum of Orion molecular Peak 1. Numerous emission lines from highly excited H_2 molecular gas of various kinematical components are detected. Currently we are trying a variety of wavelength calibration methods. We confirmed the spectral resolution by examining line widths of OH sky emission lines. We also obtained some spectra of Persson standards using the widest slit (0.6-arcsec) to confirm the throughput. It is estimated at roughly 10% including quantum efficiency (average over all the wavelength range on the array), which is close to the original estimate. However, the total throughput is highly dependent on the throughput of the slit. In particular, for the narrowest slit (0.15-arcsec) for highest spectral resolution, we need the AO system to minimize the loss of light on the slit.

5. CURRENT STATUS AND FUTURE PLAN

We plan to bring IRCS from the summit to the Subaru Hilo facility in May to check the interface to the AO system, which is planned to be delivered to the facility in April, 2000. We also plan to install the remaining order-sorting filter (L-band) as well as some narrow-band filters at that time. We plan to bring IRCS up to the summit again in July, 2000. Several engineering runs with AO and tip-tilt are scheduled in August-October. The Subaru Telescope plans to open IRCS for the public use this year as the first common-use instrument at the Cassegrain focus.

ACKNOWLEDGMENTS

We deeply appreciate support and encouragement of the entire Subaru Telescope team, in particular N. Kaifu, T. Nishimura and M. Hayashi. We thank the IRTF group at IfA, Univ of Hawaii for supporting the development of the array electronics and also kindly letting us use their hardware and software resources. We thank the Gemini NIRI development group at IfA for many useful suggestions and various collaborative works, as well as S. Massy and J. Hamilton, who kindly helped us for making spectrograph baffles with their laser cutting machine at the Gemini Observatory. We are grateful for the support before and during our first engineering run from the telescope operation group, especially T. Usuda, G. Kosugi, J. Noumaru, and T. Yamashita. We also thank T. Maihara of Kyoto University for his continuous encouragement.

[‡]With 16 slow-counts. Although smaller slow-counts (e.g., 4) enables an integration time less than 0.2 seconds, we sticked to the larger slow-counts for the first engineering run because smaller slow-conts sometimes causes an electric ghost in the row direction (readout direction) on the array.

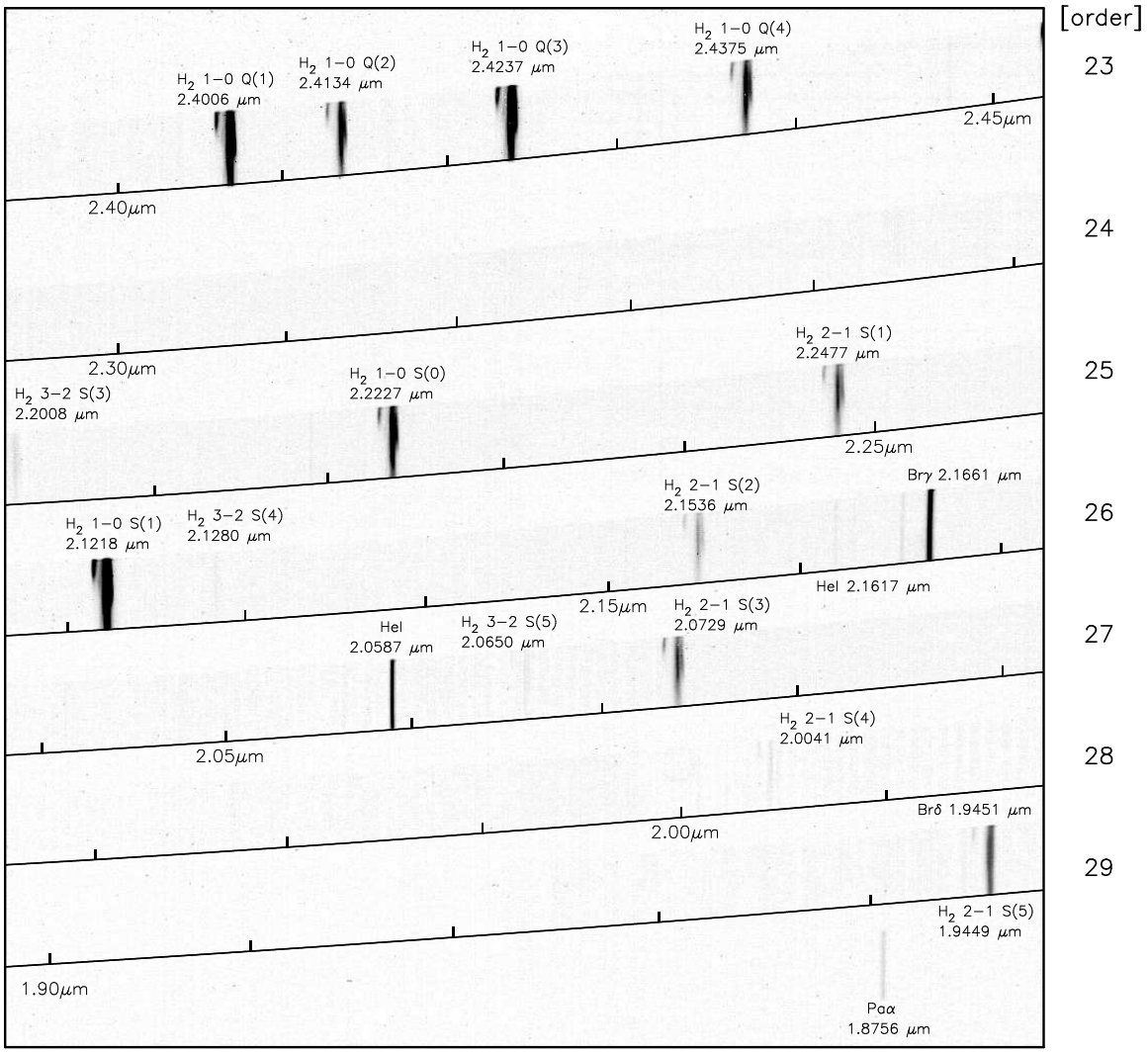

Figure 4. IRCS echelle spectrum of Orion molecular Peak 1 in K band. The shown spectrum covers about 70% of the entire K band. Taken with 0″.15 (width) × 3″.8 (length) slit with $\lambda/\Delta\lambda$=20,000.

REFERENCES

1. C. C. Steidel, "Galaxies at high redshift," in *Discoveries and Research Prospects from 8–10 Meter-Class Telescopes*, J. Bergeron, ed., *Proc. SPIE,* **4005**, 2000.
2. M. J. McCaughrean, "Star formation with large optical/IR telescopes: recent results and future prospects," in *Discoveries and Research Prospects from 8–10 Meter-Class Telescopes*, J. Bergeron, ed., *Proc. SPIE,* **4005**, 2000.
3. K. W. Hodapp, "Infrared detector arrays: current state of the art," in *Optical and IR Telescope Instrumentation and Detectors*, M. Iye and A. F. Moorwood, eds., *Proc. SPIE,* **4008**, 2000.
4. I. S. McLean, "Performance and results with the NIRSPEC Echelle spectrograph on the Keck II telescope," in *Optical and IR Telescope Instrumentation and Detectors*, M. Iye and A. F. Moorwood, eds., *Proc. SPIE,* **4008**, 2000.
5. A. F. Moorwood, "ISAAC: a 1- to 5-um imager/spectrometer for the VLT," in *Optical Telescopes of Today and Tomorrow*, A. L. Ardeberg, ed., *Proc. SPIE,* **2871**, pp. 1146–1151, 1997.

6. J. H. Elias, D. Vukobratovich, J. R. Andrew, M. K. Cho, R. W. Cuberly, K. Don, A. Gerzoff, C. F. Harmer, D. Harris, J. B. Heynssens, J. Hicks, A. Kovacs, C. Li, M. Liang, I. Moon, E. T. Pearson, G. Plum, N. A. Roddier, J. Tvedt, R. J. Wolff, and W. Wong, "Design of the Gemini near-infrared spectrometer," in *Infrared Astronomical Instrumentation*, A. M. Fowler, ed., *Proc. SPIE,* **3354**, pp. 555–565, 1998.
7. A. T. Tokunaga, N. Kobayashi, J. Bell, G. K. Ching, K. Hodapp, J. L. Hora, D. Neill, P. M. Onaka, J. T. Rayner, L. Robertson, D. W. Warren, M. Weber, and T. T. Young, "Infrared camera and spectrograph for the SUBARU Telescope," in *Infrared Astronomical Instrumentation*, A. M. Fowler, ed., *Proc. SPIE,* **3354**, pp. 512–524, 1998.
8. T. Nishimura, "Subaru Telescope: status report," in *Telescope Structures, Enclosures, Controls, Assembly/Integration/Validation, and Commissioning*, T. A. Sebring and T. Andersen, eds., *Proc. SPIE,* **4004**, 2000.
9. H. Takami, N. Takato, T. Kanzawa, Y. Kamata, K. Nakashima, and M. Iye, "Recent status of Subaru adaptive optics system," in *Adaptive Optical Systems Technology*, P. L. Wizinowich, ed., *Proc. SPIE,* **4007**, 2000.
10. T. T. Young, A. T. Tokunaga, J. L. Hora, L. Robertson, and N. Kobayashi, "Precision slit design and fabrication for the SUBARU IRCS instrument," in *Infrared Astronomical Instrumentation*, A. M. Fowler, ed., *Proc. SPIE,* **3354**, pp. 317–321, 1998.
11. J. Bell, J. W. Douglass, K. Hodapp, N. Kobayashi, L. Robertson, A. T. Tokunaga, and T. T. Young, "Design of the cryogenic wheel mechanisms for IRCS and NIRI," in *Infrared Astronomical Instrumentation*, A. M. Fowler, ed., *Proc. SPIE,* **3354**, pp. 1103–1110, 1998.
12. J. W. Douglass, T. T. Young, and K. Hodapp, "Design review of flexure focus stage for the Gemini telescope near infrared imager," in *Infrared Astronomical Instrumentation*, A. M. Fowler, ed., *Proc. SPIE,* **3354**, pp. 1062–1067, 1998.
13. P. M. Onaka, A. T. Tokunaga, N. Kobayashi, M. Weber, J. T. Rayner, A. J. Denault, D. Y. Watanabe, and G. K. Ching, "Test and selection of ALADDIN II arrays for IRCS: Redline electronics for IRCS," in *Infrared Astronomical Instrumentation*, A. M. Fowler, ed., *Proc. SPIE,* **3354**, pp. 30–38, 1998.
14. T. Usuda, K. Omata, M. Yutani, Y. Torii, Y. Mikami, T. Nishino, T. Noguchi, T. Nishimura, S. Sawada, and the Subaru Project team, "CIAX: Cassegrain Instrument Auto eXchanger for the Subaru Telescope," in *Advanced Telescope and Instrumentation Control Software*, H. Lewis, ed., *Proc. SPIE,* **4009**, 2000.
15. D. Simons, "Near Infrared Filter Bandpasses for Gemini Instruments," *Gemini Technical Notes,* **TN-PS-G0037**, 1996.
16. D. Simons, "Near Infrared Filter Manufacturing Specifications for Gemini Instruments," *Gemini Technical Notes,* **TN-PS-G0042**, 1996.
17. A. T. Tokunaga, "Infrared Astronomy," in *Allen's Astrophysical Quantities (Fourth Edition)*, A. N. Cox, ed., pp. 143–167, Springer-Verlag, New York, 2000.
18. T. Young, "Cryostat mechanism design and fabrication," in *Optical and IR Telescope Instrumentation and Detectors*, M. Iye and A. F. Moorwood, eds., *Proc. SPIE,* **4008**, 2000.
19. S. E. Persson, D. C. Murphy, W. Krzeminski, M. Roth, and M. J. Rieke, "A New System of Faint Near-Infrared Standard Stars," *Astronomical Journal,* **116**, pp. 2475–2488, 1998.